Passive Barrier as a Transformer of "Chemical Signal" Frequency

Jakub Sielewiesiuk[†] and Jerzy Górecki*[,†,‡]

Institute of Physical Chemistry, Polish Academy of Sciences, ul. Kasprzaka 44/52, 01-224 Warsaw, Poland, and ICM UW, ul. Pawińskiego 5A, 02-106 Warsaw, Poland

Received: October 17, 2001; In Final Form: January 23, 2002

We show that a passive barrier separating two excitable chemical media can work as a transformer for a frequency of a train of pulses. The results of calculations performed for the FitzHugh−Nagumo type model and for the Rovinsky−Zhabotinsky model of the Belousov−Zhabotinsky reaction are discussed. Using the Rovinsky−Zhabotinsky model, we estimate the range of barrier widths and the range of frequencies of incoming pulses for which the transforming properties may be observed.

I. Introduction

Many theoretical and experimental studies on information processing by purely chemical devices have been reported in recent years. A popular class of chemical systems that process information utilize pulses of reagent's concentration, which can be produced in excitable or oscillatory media. In the following we call such pulse a "chemical signal". Travelling pulses carry information, because the area of a high concentration of a particular reactant may be considered as corresponding to the logical "true" state, whereas the area of a low concentration corresponds to the logical "false". This idea was used to construct chemical reactors that perform the basic logical functions (AND, OR, NOT).[1,2]

More complex operations may be carried out by a system composed of "active" regions, in which reactions occur, and "passive" areas, where some of the reagents are absent, and consequently, only a part of reactions proceed there. In practice, the active areas are filled with an immobilized catalyst, while the passive areas do not contain it. A specially selected asymmetric geometry of the junction of two active areas allowed one to develop[3] and construct[4] a chemical diode, which transmits pulses only in one direction. A circular excitable field with radial input and output channels can be used as a memory cell.[5] In our recent works[6,7] we have shown that a cross junction of active and passive areas may work as a switch of direction of propagation for a "chemical signal".

The previous studies on signal processing in an excitable medium were mainly concerned with the response of the studied device to a single set of incoming pulses. Here we show that an "answer" of a chemical signal processor may be more complex if a train of incoming pulses is considered. We demonstrate that a single barrier of a passive medium separating two excitable areas works as a transformer of frequency of a chemical signal. It means that by a careful choice of the barrier's width, one can obtain an output signal containing a certain fraction of pulses from the input one.

The paper is organized as follows. In section II we introduce our system and the numerical technique used to solve the reaction−diffusion equations describing the active medium with a barrier. We also explain how the results are analyzed. Section III contains results obtained for the FitzHugh−Nagumo type dynamics. The next section is concerned with models of the Belousov−Zhabotinsky system in an excitable regime. We estimate the width of a barrier and the frequencies of chemical signals for which the transforming properties may be expected. In the final section we summarize the results.

II. Numerical Technique and Data Analysis

Let us consider an infinite plane of excitable chemical medium with a stripe of the passive medium, a barrier. In the following we consider chemical pulses in the form of planar waves, travelling perpendicularly to the stripe. Such a problem is symmetric in the direction perpendicular to the stripe, so it can be described as one-dimensional. Therefore, in our numerical simulations we model the system's evolution on a (one-dimensional) interval. A scheme of the investigated system is shown in Figure 1. The interval of length l is divided into n equal parts by $n + 1$ points of a grid, including both ends. We calculate the concentrations of reactants of interest at these points. One set of reaction−diffusion equations describes the time evolution in the active medium and another one in the passive stripe. The black areas on the line drawn at the bottom of Figure 1 correspond to the active areas, and the barrier is located between grid points n_1 and n_2 ($1 \ll n_1 < n_2 \ll n$). It means that the reaction term in the reaction−diffusion equations at all the grid points i: $i \in [0, n_1] \cup [n_2, n]$ corresponds to the active medium and for all the grid points i: $i \in (n_1, n_2)$ the reaction term describes reactions in the passive one. The barrier width is estimated as

$$d \cong (n_2 - n_1 - 1)dl \tag{1}$$

n is chosen in such a way that there are several grid points inside the passive barrier. The boundary conditions between the passive and active media correspond to a free flow of reagents between them. There are no flux boundary conditions at both ends of the interval. Initially, both active and passive areas are in their stationary states. Pulses of excitation are initiated at the left end of the interval and they travel to the right, coming across the passive barrier on their way. The method of initiating the pulses depends on the investigated model (it may be done by decreasing the inhibitor's concentration or by increasing the

* Corresponding author. E-mail: gorecki@ichf.edu.pl.
[†] Polish Academy of Sciences.
[‡] ICM UW.

10.1021/jp013844t CCC: $22.00
Published on Web 04/03/2002

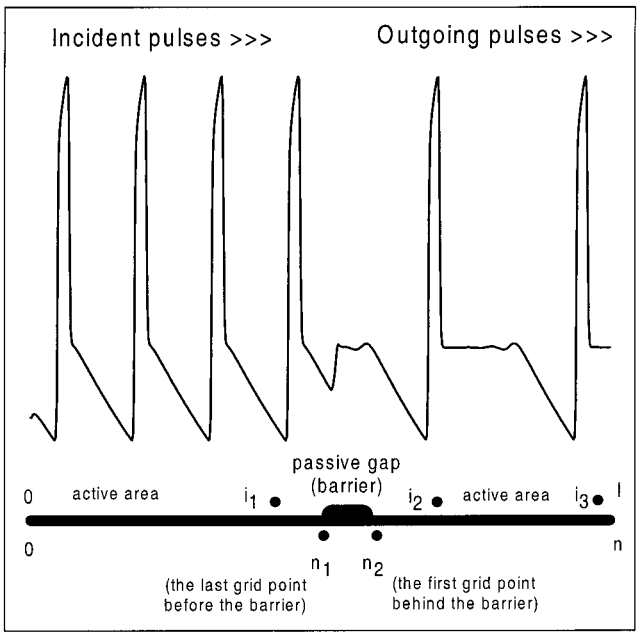

Figure 1. Scheme of the system studied. It is represented by a one-dimensional interval, shown in the bottom part of the figure; the active areas and the passive barrier are indicated. The barrier is located between grid points n_1 and n_2. Concentrations of reagents are observed at grid points i_1 (before the barrier), i_2 (just behind the barrier), and i_3 (far behind the barrier). The upper part shows a snapshot of a train of pulses propagating in the system (incoming signal, on the left-hand side and outgoing signal, on the right-hand side). Let us notice that the signals have different frequencies.

concentration of activator) and we describe it in detail in the following sections. We focus our attention on trains of pulses that are initiated regularly at times kt_p, where $k = 1, 2, 3, ..., k_{max}$ and $t_p > 0$ is a constant.

To study the filtering properties of the barrier, we introduce two "indicators" that measure the concentrations of reagents at the grid point $i_1 = n_1 - 2$ (before the barrier) and at the grid point $i_2 = n_2 + 2$ (just behind the barrier). By comparing the time evolution of concentrations at these points, we can see whether every signal that arrives at the barrier is able to cross it. Moreover, by counting the number of maxima of concentration within a certain time interval, we can measure the frequency of the incoming and outgoing chemical signals. To observe the further evolution of the outgoing signal, we introduce another indicator i_3, located far behind the barrier (cf. Figure 1).

The implicit method based on the Crank−Nicolson discretization of the Laplace operator[8] has been applied to integrate the reaction−diffusion equations numerically. The distance between neighboring grid points ($dl = l/n$) is the step of numerical integration. In calculations we usually take n between 200 and 300, but computations for a larger number of grid points have been also performed in order to check the numerical stability of results.

If only a single pulse propagating in the excitable area toward the barrier is considered, then nothing especially interesting can happen in a one-dimensional system. If the barrier is narrow, it is transparent to the pulse, which means that the pulse arriving at one side of it excites the active area on the other side. If the barrier is wide, the pulse does not get through it. The maximum width of a transparent barrier is called the penetration depth.

The problem of penetration through the barrier becomes more interesting if we consider a train of arriving pulses. Discussing the properties of selected models we show that two scenarios are possible. For one model, a passive barrier transparent to the first pulse may be impenetrable for the next one. For another, the first of arriving pulses which is stopped by a barrier wider than the penetration depth, may "open" it to the subsequent pulses. Both types of behavior are illustrated in Figure 2A−C, which show the time evolution of activator's concentration at the grid point i_1 (the upper curve (1)) and at the grid point i_2 (curves 2−4). In addition, curve 5 in Figure 2A shows the evolution at the grid point i_3, far behind the barrier. The evolution at the initial stage of the process is given. The time scale starts just before the first pulse of the train arrives at the barrier. Parts A−C of Figure 2 correspond to the FitzHugh−Nagumo model (FH−N), Rovinsky−Zhabotinsky model (R−Z), and the Oregonator model discussed in the following sections. Three lower curves show the evolution for the following cases: (2) no barrier in the system, (3) a narrow passive barrier, which is fully transparent, and (4) a barrier of an appropriate width, for which the frequency of the outgoing signal is different from the incoming one. Curve 5 in Figure 2A is presented to ensure that the small maxima of concentration seen on curve 4 (Figure 2A) do not develop into pulses.

The results for the FH−N model (eqs 2−5) and the barrier of width $d = 0.165$ (Figure 2A, curves 4 and 5) show that the first arriving pulse is stopped, the second pulse goes through the barrier, and the next every odd pulse is stopped and every even transmitted. Therefore the outgoing signal's frequency is half of the original one. We can say that an earlier pulse "opens" the barrier for the next one.

The reverse behavior is observed for both R−Z and the Oregonator models of the Belousov−Zhabotinsky (BZ) system. For these models the first arriving signal is transmitted, but a number of subsequent ones may be stopped, depending on the barrier's width, so in this case the earlier pulse passes through and "closes" the barrier. Figure 2B, curve 4, shows the outgoing signal with one-third of the original frequency (R−Z model, eqs 6−9), whereas Figure 2C, curve 4, demonstrates the barrier, which divides the original number of pulses for BZ system by two (the Oregonator model, eqs 24−27).

To describe qualitatively the properties of a passive barrier, we consider a train of many (usually about a hundred) pulses with a constant time shift t_p between them. We measure the frequency of pulses in front of the barrier (f_1) and behind it (f_2). Calculations have been performed for different values of t_p and different values of the barrier width d. We have found regimes for which the ratio f_1/f_2 is a small integer number j, which corresponds to a systematic transmission of every jth pulse from a train through the barrier. To avoid transient effects in the signal analysis, we neglect a small number (around 10) of initial pulses arriving at the first indicator (grid point i_1 in Figure 1) when calculating f_1 and f_2. The diagrams in the space of parameters (d, t_p) showing "phases" in which the barrier transforms a chemical signal in a given way are shown in figures describing results obtained for particular models.

We think that d and t_p (or f_1) are the proper variables to describe how a passive barrier works as a transformer of the signal frequency. The interval of t_p (or f_1) is limited by the fact that once the excitable medium has been excited it needs some minimal amount of time (called the refractory period) in order to relax, before it may be excited again. Thus, there exists a minimal time pace $t_{p,min}$ at which the pulses can be successfully initiated. The time $t_{p,min}$ depends on the strength of excitation and it fixes the upper frequency of the signal. On the other hand making t_p very long reduces the problem to the propagation of a single pulse. The range of d is also finite as there always

exists a barrier of width d_{min} narrow enough to be transparent to all pulses in a train and another one impenetrable for any of them (with a width of d_{max}). Thus the nontrivial transforming properties of the passive barrier may be observed only in some finite range of t_p and d, which depends on the selected model and values of its parameters.

III. The FitzHugh−Nagumo Model

In this section we consider a system for which the dynamics in the active areas is described by a simple FitzHugh−Nagumo type model:[3,9,10]

$$\tau\frac{\partial u}{\partial t} = -\gamma[ku(u-\alpha)(u-1)+v] + D_u\nabla^2 u \qquad (2)$$

$$\frac{\partial v}{\partial t} = \gamma u \qquad (3)$$

with the parameters $\tau = 0.03$, $\gamma = 1$, $k = 3.0$, $\alpha = 0.02$ (as given by Motoike and Yoshikawa in ref 3), and $D_u = 0.00045$.[6] For these values of parameters the system has one stationary solution $(u, v) = (0, 0)$, which is excitable. The variables u and v cannot be directly associated with concentrations of chemical spices, but their behavior resembles the one of the activator (u) and inhibitor (v).

We assume that in the passive area no reaction occurs and only diffusion of activator is possible, thus it is natural to call this region a "diffusion area". The equations describing the time evolution of u and v in this area are[3]

$$\tau\frac{\partial u}{\partial t} = D_u\nabla^2 u \qquad (4)$$

$$v = 0 = \text{const} \qquad (5)$$

with $\tau = 0.03$ and $D_u = 0.00045$, as in the excitable areas.

In calculations for this model the following parameters have been used: $n = 251$, $n_1 = 150$, $n_2 = 160$. To produce a pulse, the value of v has been decreased to $v_{ini} = -0.2$ on the left end of the interval. Using the time integration step $dt_1 = 5 \times 10^{-3}$, we have found that a single pulse is able to cross the passive barrier for $d = 0.1631$, but for $d = 0.1635$ the barrier becomes impenetrable. This means that the penetration depth in the FitzHugh−Nagumo system is about $d_{max,FH-N} \approx 0.163$.

For the considered values of parameters, the minimum time after which the second pulse may be re-excited is $t_{p,min,FH-N} \approx 2.4$. However, for such a short time of consecutive excitations it is not possible to obtain a regular, stable train of pulses, because it happens that the medium at the initiation point is not well relaxed and an attempt to re-excite it by the assumed v_{ini} fails. For the FitzHugh−Nagumo system the value of $t_{p,min,FH-N}$ strongly depends on v_{ini} (the strength of excitation) and also on dl, which describes the spatial size of excitation. In our calculations in order to create a stable train of pulses we have used $t_p \in [2.90, 4.04]$.

The maximum time within which the evolution is studied (t_{max}) is fixed in our calculations. The system is excited approximately $p = t_{max}/t_p$ times, so it is expected that such number of pulses is produced. We can check it by counting the number of pulses p_1 that reach the first indicator during that time. The ratio: p_1/p is called the initiation ratio. If it is remarkably smaller than 1, we know that not all attempts of initiating a pulse are successful. On the other hand, when it is close to 1, we obtain nice regular trains of pulses and only such cases are considered below. The time shift between individual pulses within a regular train equals t_p and $f_1 = 1/t_p$ gives the frequency of incident pulses at the first indicator.

To investigate the effect of the barrier, we have used $t_{max} = 500$ and the time integration step $dt_1 = 5 \times 10^{-3}$ to study a range of t_p from 2.98 to 4.04 with increments 0.02 ($f_1 \in [0.248, 0.336]$) and the barrier widths $d \in [0.126, 0.172]$. For the selected t_{max} and t_p we have observed from 120 to 160 pulses in the system for each combination of t_p and d.

Figure 2A presents a sample signal (concentration of u) observed at the grid points $i_1 = 148$, $i_2 = 162$, and $i_3 = 248$ for $dl = 0.0175$, $n = 251$, and $f_1 = 0.294$. For all the results shown in Figure 2A $n_1 = 150$, while n_2 is changed to obtain barriers of a various width d. The upper curve (1) corresponds to incident pulses (reference signal at indicator i_1). In case of $n_2 = 151$ (no passive barrier) the same signal is observed at indicator i_2 with only a small time shift, which the signal needs to cover the distance between indicators i_1 and i_2 (signal at i_2, curve 2). The result is the same for $n_2 = 155$, which corresponds to a thin, fully transparent passive barrier (curve 3 presents the signal at i_2). All incident pulses observed at indicator i_1 get through the barrier and are also observed at indicator i_2. However, for a properly chosen width the barrier becomes selective. For $n_2 = 160$ (the barrier's width is then $d = 0.158$) exactly every second of the incident pulses is transmitted through the barrier and observed at indicator i_2 (curve 4) or indicator i_3 (curve 5).

Figure 3 summarizes the signal transforming properties of a passive barrier as a function of the barrier's width d and the time shift between consecutive incident pulses t_p. The regions of the same color correspond to a given ratio of frequencies (f_2/f_1) of the outgoing (f_2) and incoming (f_1) trains of pulses, called a filtering ratio. The area labeled as "1" indicates the ratio equal to 1, which means that every incident pulse is able to get through the passive barrier (the barrier is transparent to all pulses). When t_p decreases, we arrive at the area (labeled as "1/2" in Figure 3) where only every second of the incident pulses is transmitted. Increasing d, we observe that the filtering ratio decreases, which means that the pulses are less and less frequently transmitted (see area "1/3" in Figure 3, where only one out of three of incident pulses gets through the barrier). Finally, the barrier becomes too wide and no pulse can cross it (thus $f_2 = 0$). This corresponds to the area labeled as "0" in Figure 3. The hatched regions between the labeled areas in Figure 3 correspond to more complex (periodic or nonperiodic) transmission patterns (cf. Figure 5, described later in text).

The dark area below the region "1/2" corresponds to the cases in which the excitation by $v_{ini} = -0.2$ does not lead to a regular train of pulses with the frequency $f_1 = 1/t_p$, because some attempts at excitations fail. We have repeated the calculations for different methods of pulse initiation (for example using $v_{ini} = -0.4$) and for a different number of grid points ($n = 300$). For stronger excitations we are able to obtain a regular train of pulses with frequency $f_1 = 1/t_p$ for the whole range of t_p and d shown in Figure 3. The calculations have shown that for a given t_p, for which every excitation is successful and for a selected d the observed type of behavior and the filtering ratio do not depend on the method of excitation. For $v_{ini} = -0.4$ all points that belong to the dark area in Figure 3 fall into the "1/2" region. Nevertheless, in Figure 3 we marked them with a dark color, just to indicate problems with periodic excitations.

We have studied more carefully the part of the parameter space for which the filtering ratio is smaller than 1. We have used $t_{max} = 500$ and $dt_2 = 2 \times 10^{-3}$ and investigated the range of t_p from 3.00 to 3.40 with increments of 0.01 and the range of d from 0.168 to 0.173 with increments of 0.00018 (this is

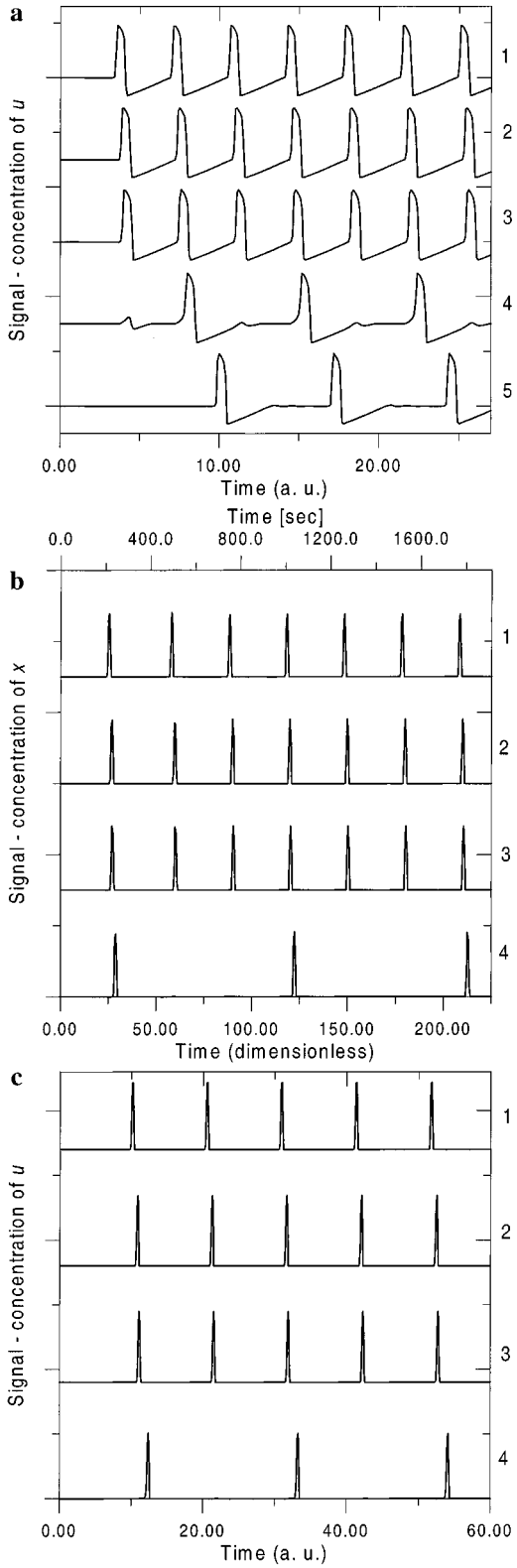

Figure 2. Time evolution of activator's concentration at grid point i_1 (the upper curve 1), at grid point i_2 (curves 2−4), and at grid point i_3 far behind the barrier (curve 5). The evolutions at i_2 correspond to no barrier (curve 2), a narrow transparent barrier (curve 3), and to a barrier for which frequency transformation occurs (curve 4). In the last case the evolution at i_3 is also shown (curve 5). (A) FitzHugh−Nagumo model (eqs 2−5), $t_p = 3.40$ ($f_1 = 0.294$), $d = 0.070$ (curve 3), $d = 0.158$ (curves 4 and 5). (B) Rovinsky−Zhabotinsky model (eqs 6−9), $\tau_p = 30$ ($f_1 = 0.033$), $d = 1.628$ ($0.0150\sqrt{D_X/D_{X_0}}$ cm) (curve 3), $d = 3.256$ ($0.0300\sqrt{D_X/D_{X_0}}$ cm) (curve 4). $\tau_p = 30$ corresponds to 255 s. (C) Oregonator model (eqs 24−27), $t_p = 10.4$ ($f_1 = 0.096$), $d = 1.867$ (curve 3), $d = 3.733$ (curve 4).

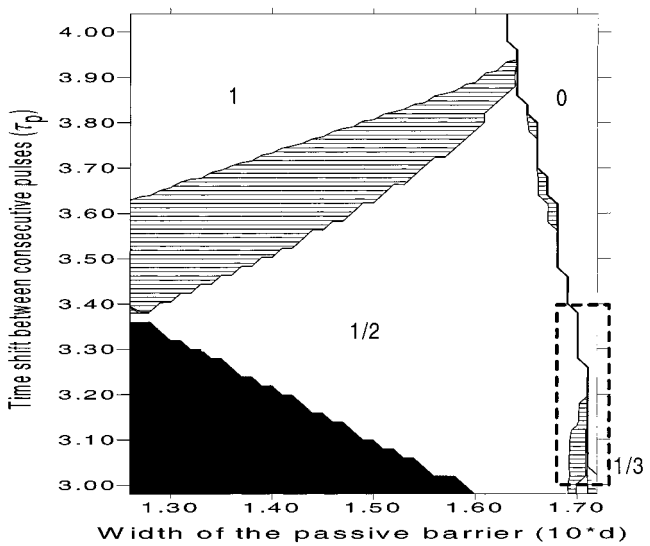

Figure 3. Filtering ratio (f_2/f_1) for the FitzHugh−Nagumo model as a function of the barrier's width (d) and the time shift between consecutive incident pulses (t_p). The white, labeled areas correspond to the situation when f_2 is the given fraction of f_1. The dark area in the bottom left-hand side corner indicates the region of parameters where not all excitations lead to a pulse. The hatched area marks more complicated transformations of frequency. The rectangular area in the bottom right-hand side corner of the picture has been studied more carefully and is illustrated in Figure 4.

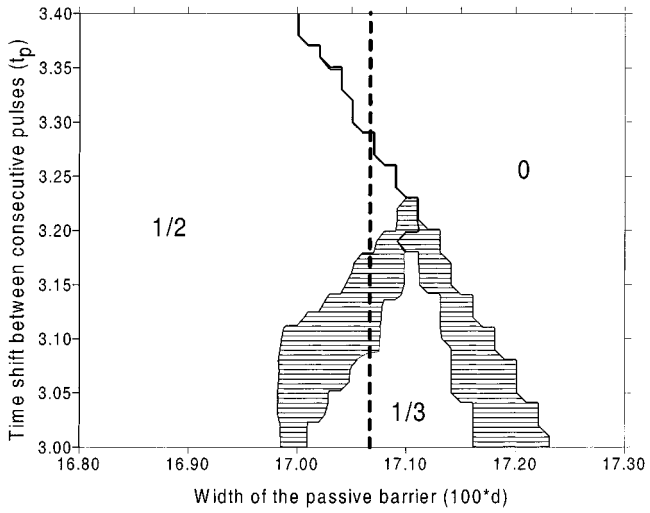

Figure 4. Filtering ratio (f_2/f_1) for the FitzHugh−Nagumo model as a function of the barrier's width (d) and the time shift between consecutive pulses (t_p). The white, labeled areas correspond to the situation when f_2 is the given fraction of f_1. Hatched areas stand for more complicated transformations of frequency. The dashed line indicates $d = 0.1707$.

the rectangular area marked with dashed line in the bottom right-hand side corner of Figure 3). The results are presented in Figure 4, for which the meaning of the colors and labels is the same as in Figure 3.

We have found that the filtering ratio equal to 1/2 is dominant among the nontrivial filtering. In most cases it means that the barrier eliminates every second pulse from the train. The "scenario" of such elimination for the FitzHugh−Nagumo model is shown in Figure 2A. It shows that the first incident pulse "dies" at the barrier, but the next one is transmitted, another one dies, etc. Similar observation is valid for lower values of the filtering ratio. For example in the case of filtering ratio equal to $^1/_3$, the first and second incident pulses die and the third one is transmitted. We think that a pulse stopped at the barrier

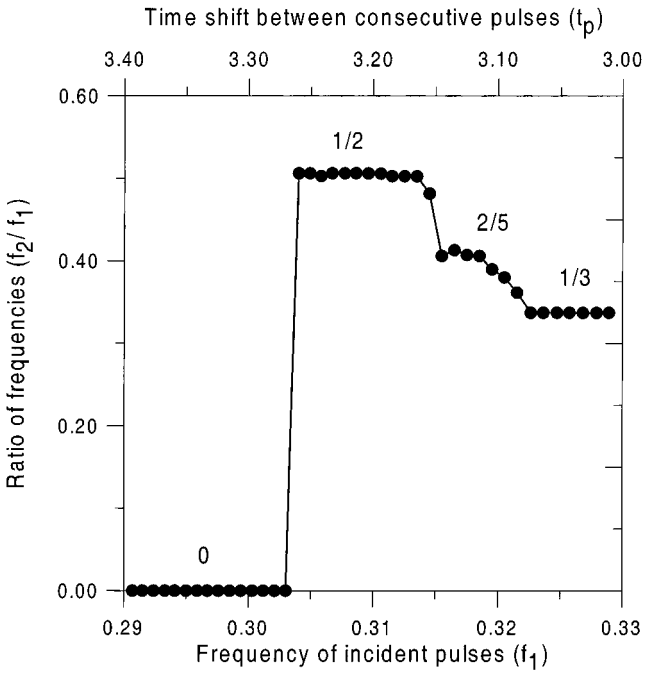

Figure 5. Filtering ratio in the FitzHugh−Nagumo model for a selected barrier's width $d = 0.1707$. f_2/f_1 is presented as a function of the frequency of incident pulses (f_1, bottom axis) or the (approximate) time shift between consecutive incident pulses (t_p, top axis). Labels describe the filtering ratio (f_2/f_1).

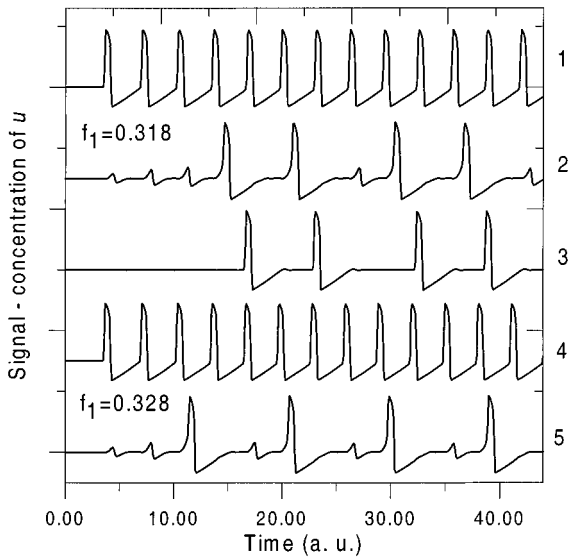

Figure 6. Time evolution of activator's concentration in the FitzHugh−Nagumo model at indicator 1 (grid point i_1, before the barrier, curves 1 and 4), at indicator 2 (grid point i_2, just behind the barrier, curves 2 and 5), and at indicator 3, far behind the barrier (curve 3) for $d = 0.1707$. Curves 1−3 correspond to $f_1 = 0.318$ and illustrate the frequency transforming ratio equal to 2/5. Curves 4 and 5 correspond to $f_1 = 0.328$ and illustrate the frequency transforming ratio equal to 1/3.

increases the value of u inside the barrier for a short period of time, so the "activator" is accumulated within the passive area. This helps the next incident pulse to get through the barrier.

Let us also notice that there are hatched regions in Figures 3 and 4, which separate the areas labeled as "1", "1/2", "1/3". In these regions of the parameters' space (d, t_p) the transformation of the frequency of incoming train of pulses is more complex. An example is shown in Figure 5, which presents the filtering ratio f_2/f_1 versus the frequency of incident pulses f_1 for a selected barrier width $d = 0.1707$. This value of d is indicated by a thick black line in Figure 4. If f_1 is smaller than 0.303, no pulse is transmitted and so f_2 is zero. The selected barrier is wider than a penetration depth, so if the time separation between pulses t_p is large, they behave like individual ones and they are not able to cross the barrier.

For $f_1 > 0.303$ the barrier opens to every second of the arriving pulses. The evolution is the same as shown in Figure 2A (curves 1, 4, and 5) and every second pulse is transmitted until the frequency f_1 reaches 0.313. At this point the filtering ratio drops from 1/2 to 0.4. Such a ratio seems to be stable in a narrow range of $f_1 \in (0.316, 0.319)$. It corresponds to a more complex behavior illustrated in Figure 6 (curves 1−3). Results presented in Figure 6 have been obtained for $n = 251$, $dl = 0.01896$, $n_1 = 150$, and $n_2 = 160$ (so the barrier's width is $d = 0.1707$). Indicators are located at grid points $i_1 = 148$, $i_2 = 162$, and $i_3 = 248$. Curves 1−3 show the signal at indicators i_1, i_2, and i_3 respectively, for $f_1 = 0.318$ ($t_p = 3.14$). Let us notice that just after crossing the barrier the signal has the period of $5t_p$ with two maxima of concentration per period (Figure 6, curve 2). The signal far behind the barrier is shown as the curve 3. One can see that the small maxima have not developed into the regular pulses and the signal is composed of peaks separated by $2t_p$ and $3t_p$. We believe that such form of a signal has a transient character. The numerical experiments with pulses in the FH−N system have indicated that a velocity of a pulse increases with the distance separating it from the preceding ones.[11] Thus, a pulse that propagates $3t_p$ after the preceding ones is faster than that propagating $2 \cdot t_p$ after the preceding ones. In the long time limit one obtains a periodic signal, the frequency of which is 2/5 of the original one. The stability of the 2/5 filtering mode described here has been confirmed by calculations carried out up to $t_{max} = 10000$. We observe that the increment of f_1 leads to more complex output (Figure 5), which requires further studies. A further increase in frequency leads to the output signal for which $f_2 = f_1/3$. The region "1/3" continues to the highest frequencies for which a regular train of pulses may be created. Such behavior is illustrated in Figure 6 by curves 4 (signal at i_1) and 5 (signal at i_2) for $f_1 = 0.328$.

IV. Models of Chemical Systems: The Rovinsky−Zhabotinsky and the Oregonator Model

In this section we present the filtering properties of a passive barrier in an excitable medium described by models that can be associated to a real chemical reaction.

We have focused our attention on the Rovinsky−Zhabotinsky model of the Belousov−Zhabotinsky reaction,[12,13] which is based on the Field−Körös−Noyes[14,15] mechanism of the Belousov−Zhabotinsky reaction[13] completed by the hydrolysis of bromomalonic acid to tartronic acid.[12] The Rovinsky−Zhabotinsky model uses two variables: x and z, corresponding to dimensionless concentrations of the activator $HBrO_2$ and of the oxidized form of catalyst $Fe(phen)^{3+}{}_3$. In the active regions, which contain the catalyst, the time evolution of the concentrations of x and z is described by

$$\frac{\partial x}{\partial \tau} = \frac{1}{\epsilon}\left[x(1-x) - \left(2q\alpha\frac{z}{1-z} + \beta\right)\frac{x-\mu}{x+\mu}\right] + \nabla_\rho{}^2 x \quad (6)$$

$$\frac{\partial z}{\partial \tau} = x - \alpha\frac{z}{1-z} \quad (7)$$

In the passive region, without catalyst, the concentrations of x

and z evolve according to

$$\frac{\partial x}{\partial \tau} = -\frac{1}{\epsilon}\left[x^2 + \beta\frac{x-\mu}{x+\mu}\right] + \nabla_\rho{}^2 x \tag{8}$$

$$z = 0 = \text{const} \tag{9}$$

Equations 6−9 correspond to a typical experimental situation in which the catalyst is immobilized on a membrane, whereas the activator is in the solution and it can diffuse (compare refs 4 and 16). Therefore, we assume free boundary conditions between the active and passive areas.

All variables and coefficients in eqs 6−9 are dimensionless. The real concentrations of $HBrO_2$ and $Fe(phen)^{3+}{}_3$ (X, Z) are related to (x, z) in the following way:

$$X = \frac{k_1 A}{2k_4}\, x \tag{10}$$

$$Z = Cz \tag{11}$$

The coefficients (α, β, μ, ϵ) are defined as

$$\alpha = \frac{k_4 K_8 B}{k_1{}^2 A^2 h_0{}^2} \tag{12}$$

$$\beta = \frac{2k_4 k_{13} B}{k_1{}^2 A^2 h_0} \tag{13}$$

$$\mu = \frac{2k_4 k_7}{k_1 k_5} \tag{14}$$

$$\epsilon = \frac{k_1 A}{k_4 C} \tag{15}$$

where $k_{\pm i}$ denote the rate constants of the corresponding reactions in the Field−Körös−Noyes model[12−15] and $A = [HBrO_3]$, $B = [CHBr(COOH)_2]$, $C = [Fe(phen)^{2+}{}_3] + [Fe(phen)^{3+}{}_3]$, $R = [^{\cdot}CBr(COOH)_2]$, $U = [HBrO^+{}_2]$, $X = [HBrO_2]$, $Y = [Br^-]$, $Z = [Fe(phen)^{3+}{}_3]$, and q is the stoichiometric factor. Parameter h_0 denotes the Hammett acidity function, describing the effective proton concentration[17−19] and it is expressed in mol/L.

In our numerical calculations for the BZ system we use the same values of parameters as considered in refs 12, 13, and 20: $A = 0.02$ M, $B = 0.2$ M, $C = 0.001$ M, $k_1 = 100$ M^{-2}/s, $k_4 = 1.7 \times 10^4$ M^{-2}/s, $k_5 = 10^7$ M^{-2}/s, $k_7 = 15$ M^{-2}/s, $K_8 = 2 \times 10^{-5}$ M/s, $k_{13} = 10^{-6}$ s^{-1}, $q = 0.5$. The corresponding values of scaled parameters α, β, ϵ, μ are $0.017h_0{}^{-2}$, $0.0017h_0{}^{-1}$, 0.1176, and 0.00051, respectively. For these values of parameters the system becomes excitable if $h_0 < 0.9899$.[20] As in ref 7 we have chosen $h_0 = 0.5$.

Equations 6−9 are written in the dimensionless units of time τ and distance ρ. The relationships between them and the real time t and distance r are the following:

$$t = \frac{k_4 C}{k_1{}^2 A^2 h_0}\cdot\tau \tag{16}$$

$$r = \sqrt{\frac{k_4 C}{h_0}}\,\frac{1}{k_1 A}\sqrt{D_X}\cdot\rho \tag{17}$$

where D_X is the diffusion constant of the activator x. For the parameters chosen

$$t\ (\text{s}) = 8.5\tau \tag{18}$$

$$r\ (\text{cm}) = 2.915\sqrt{D_X\ (\text{cm}^2/\text{s})}\,\Delta\rho \tag{19}$$

However, the diffusion constant strongly depends on the medium in which the reactions proceed. In the aqueous solution it is of the order of 10^{-5} cm^2/s,[4,12,17,19,20] whereas for a reaction in a gel it may be reduced by 2 orders of magnitude.[4,21] To make our results more general, we present all distances and velocities in the double form: dimensionless and as the function of the ratio of diffusion constants D_X/D_{X_0}, where the value of D_{X_0} corresponds to a particular choice of the diffusion constant: $D_{X_0} = 1 \times 10^{-5}$ cm^2/s.[12,20] The second number allows to see more clearly the real spatial and temporal scale of the considered process.

For the values of parameters defined above the stationary concentrations of x and z in the active areas are

$$x_{sa} = 7.283 \times 10^{-4} \tag{20}$$

$$z_{sa} = 1.060 \times 10^{-2} \tag{21}$$

(which is the stationary solution of eqs 6 and 7) and the stationary concentrations in the passive area (the stationary solution of eqs 8 and 9) are given by

$$x_{sp} = 5.100 \times 10^{-4} \tag{22}$$

$$z_{sp} \equiv 0 \tag{23}$$

In our calculations for the Rovinsky−Zhabotinsky model we have used $n = 320$, $n_1 = 150$, $n_2 = 155$ and the dimensionless time integration step $d\tau = 1 \times 10^{-3}$. The pulses are initiated at the left end of the interval by increasing the value of x to 0.1. We have found that the penetration depth for a single pulse is about 3.295 ($0.03037\sqrt{D_X/D_{X_0}}$ cm). This value is close to the one given in ref 7, but we believe that the present estimation is more accurate due to a better method of numerical integration (in ref 7 the Euler explicit method was used).

Figure 2B presents a typical signal (value of x) observed at the first and second indicators (grid points i_1 and i_2) for $dl = 0.814$ ($n = 320$) and $\tau_p = 30.0$ (255 s). For those values of parameters the excitation at the boundary gives a regular and stable train of pulses. In all calculations the results of which are shown in Figure 2B, $n_1 = 150$ and the indicators are located at grid points $i_1 = 148$ and $i_2 = 157$, while n_2 is changed to obtain barriers of a different width. The upper curve (1) corresponds to incident pulses (reference signal at indicator 1). For $n_2 = 151$ (no passive barrier, curve 2) the same signal (shifted in time) is observed at indicator 2. The same behavior is observed for a thin, fully transparent passive barrier ($n_2 = 153$, curve 3). All incident pulses observed at indicator 1 get through the barrier and are also observed at indicator 2. For $n_2 = 157$ every third of the incident pulses is transmitted through the barrier as it is observed at indicator 2 (curve 4). In this case the width of the passive barrier is 3.256 ($0.0300\sqrt{D_X/D_{X_0}}$ cm). Let us also notice that unlike for the FH−N model, the passive barrier in the R−Z (BZ) system is transparent to the first arriving pulse and it may become closed for the subsequent ones. Therefore the transformation of frequency occurs for barriers which are narrower than the penetration depth.

For the parameters of R−Z model we observe that the minimal time necessary to initiate a new pulse after the first

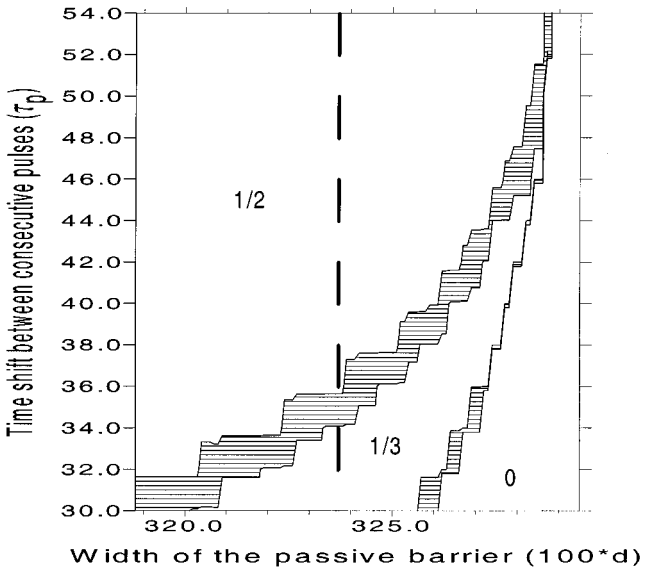

Figure 7. Filtering ratio (f_2/f_1) for the Rovinsky−Zhabotinsky model as a function of the barrier's width (dimensionless, d) and the time shift between consecutive pulses (dimensionless, τ_p). The white, labeled areas correspond to the situation when f_2 is the given fraction of f_1. Hatched areas stand for more complicated transformations of frequency. The dashed line indicates $d = 3.2375$.

pulse has been produced in the system is $\tau_{p,min,RZ} \approx 5.8$ (49 s) but one has to use much higher values of τ_p to obtain a stable, regular train of pulses. We have studied the range of τ_p from 30 (255 s) to 60 (510 s) with increments of 2 (17 s) and considered d changing from 3.188 ($0.02939 \cdot \sqrt{D_X/D_{X_0}}$ cm) to 3.295 ($0.03037 \cdot \sqrt{D_X/D_{X_0}}$ cm). $\tau_{max} = 2000$ (17000 s) has been used, so during the evolution from 33 up to 66 pulses may appear in the system for each combination of τ_p and d.

The results are shown in Figure 7. For all the examined values of d and τ_p every excitation creates a pulse. The filtering ratio f_2/f_1 presented in Figure 7 reveals areas of parameters' values for which every second or every third of the incident pulses is transmitted (those regions are labeled as "1/2" and "1/3", respectively). We have noticed that the "scenario" here is different than the one for the FitzHugh−Nagumo model, although the overall effect is the same. In contrary to FitzHugh−Nagumo, for the Rovinsky−Zhabotinsky model the stable elimination of every second pulse from a train means that the first incident pulse crosses the barrier, the next one "dies", etc. For division by 3, the first pulse gets through and then two pulses "die", etc. (cf. Figure 2B). This suggests that the mechanisms of crossing the passive barrier are different in the two discussed models. Label "0" in Figure 7 indicates the area in which no pulse can cross the passive barrier. The hatched regions between the white, labeled areas in Figure 7 correspond to more complex transmission patterns.

Figure 8 presents the filtering ratio f_2/f_1 plotted versus the frequency of incident pulses f_1 for a selected barrier width $d = 3.2375$ ($0.0298\sqrt{D_X/D_{X_0}}$ cm). This value of d corresponds to the thick dashed vertical line in Figure 7. Here the frequencies f_1 and f_2 are dimensionless frequencies, calculated as the inverse of dimensionless time τ. For $f_1 \in [0.0167, 0.0278]$ every second of incident pulses gets through the barrier. For $f_1 \geq 0.0294$ only one out of three incident pulses gets through the barrier (thus we have the filtering ratio $f_2/f_1 = 1/3$).

To check if the frequency transforming is a typical feature of a passive barrier in an excitable medium, we have performed calculations for the Oregonator model[22−24] in the form presented

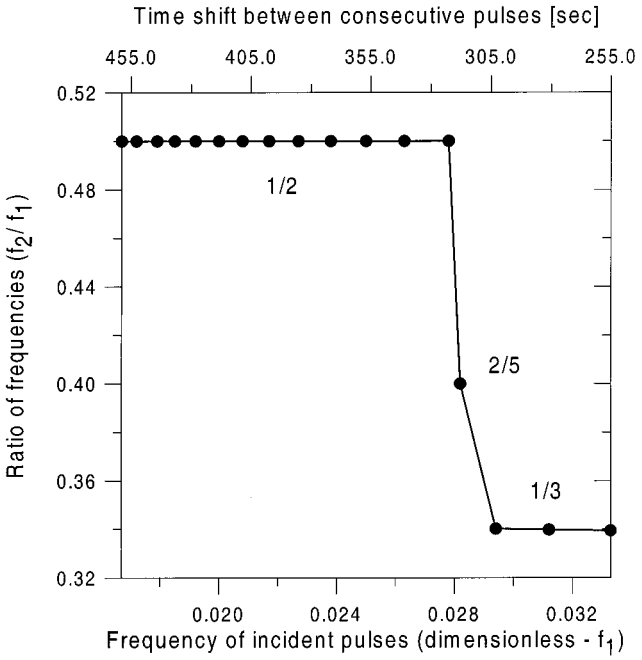

Figure 8. Filtering ratio in the Rovinsky−Zhabotinsky model for a selected barrier's width $d = 3.2375$ ($0.0298\sqrt{D_X/D_{X_0}}$ cm). f_2/f_1 is presented as a function of the dimensionless frequency of incident pulses (f_1, bottom axis) or the (approximate) physical time shift between consecutive incident pulses (t_p (s), top axis). Labels give the filtering ratio (f_2/f_1).

in ref 23 with diffusion of the activator added. In the Oregonator model the active field is described with the following reaction−diffusion equations:

$$\frac{\partial u}{\partial t} = \frac{1}{\epsilon}\left[u(1-u) - f v \frac{u-q}{u+q}\right] + D\nabla^2 u \tag{24}$$

$$\frac{\partial v}{\partial t} = u - v \tag{25}$$

where u corresponds to the scaled concentration of activator ($HBrO_2$) and v, to the scaled concentration of catalyst (Ce^{4+}).[23] In the passive regions, without catalyst, the concentrations of u and v evolve according to

$$\frac{\partial u}{\partial t} = -\frac{1}{\epsilon}u^2 + D\nabla^2 u \tag{26}$$

$$v = 0 = \text{const} \tag{27}$$

In eqs 24−27 t stands for the scaled time and ϵ (a time scale parameter) is small.[23] Another small parameter q is connected to the rate constants of the reactions involved in the Oregonator model. The stoichiometric parameter f is proportional to the average number of bromide ions released per metal ion reduced by organic matter. The details of scaling are described in ref 23.

In our calculations we have used $\epsilon = 0.05$,[24] $f = 3$,[23] $q = 0.0002$,[23] and $D = 1.0$. For these values of parameters the stationary state of the system within the active areas corresponds to

$$u_{sa} = v_{sa} = 3.9988 \times 10^{-4} \tag{28}$$

and it is excitable. In the passive areas the stationary solution

is given by

$$u_{sp} = v_{sp} \equiv 0 \tag{29}$$

In our calculations for this model we have used the implicit method described in section II with $dl = 0.3733$ ($n = 400$), $n_1 = 200$, $dt = 1 \times 10^{-4}$, and $t_p = 10.4$. The pulses have been initiated on the left end of the interval by decreasing v to $v_{ini} = 0.0$. The evolution of this system has been studied up to $t_{max} = 1000.0$ (so that over 95 pulses is involved in each experiment). We have observed that the filtering properties of a passive barrier in the Oregonator model are similar to those for FH−N and R−Z models. Figure 2C presents a sample signal (the value of u) observed at the first and second indicators (grid points $i_1 = 198$ and $i_2 = 213$, respectively). As mentioned above, $n_1 = 200$ while n_2 is changed to obtain barriers of different width. The upper curve (1) corresponds to incident pulses (reference signal at indicator 1). For $n_2 = 201$ (no passive barrier, curve 2) the same signal (shifted in time) is observed at indicator 2. The same behavior is observed for a thin, fully transparent passive barrier ($n_2 = 206$, curve 3). All incident pulses observed at indicator 1 get through the barrier and are also observed at indicator 2. For a wider barrier ($n_2 = 211$) every second of the arriving pulses is transmitted through the barrier and may be observed at indicator 2 (curve 4). For this curve the width of the passive barrier is 3.733. In this case, as for R−Z (BZ) system, the frequency is transformed for a barrier narrower than the penetration depth, because the first transmitted pulse makes the barrier impenetrable for the subsequent ones.

V. Conclusions

In the paper we discuss the properties of a barrier in the form of a stripe of a passive area separating two regions of space in which the system is in the excitable regime. We have studied the evolution of a train of regularly created pulses of excitation, which arrive at such a barrier. Our investigation is based on numerical solution of the corresponding reaction−diffusion equations with the free flow of mobile reagents between the active and passive regions.

Two facts are obvious: if the barrier is narrow, it is transparent to the pulses; if it is wide, it is impenetrable. However, we have found that between these two limiting cases there is a range of barrier widths for which it works as a transformer of signal's frequency. It means that every second, third, etc. pulse from the incoming signal is transmitted and all the others are stopped at the barrier. The number of transmitted pulses decreases with the barrier's width. We have also observed more complex examples of signal transformation, like, e.g., a selection of two pulses out of every five arriving, shown in Figure 6. Unfortunately, such interesting, complex behavior occurs in a narrow range of barrier widths and it is not as robust as a simple division of the number of input pulses by two or three. As shown in Figure 7 the division of the original frequency by 2 within the R−Z model occurs in a wide range of parameters' values, so we believe the effect can be easily studied experimentally.

The calculations have been performed for the FH−N model of an excitable system as well as for the R−Z and Oregonator models of the ferroin/cerium catalyzed BZ reaction. For all these models we have found an interval of barrier's width in which the barrier works as a transformer of frequency of the input signal. We have also found that the mechanisms of the signal transformation for the FH−N model and for the models of BZ reaction are different. In the former case the signal transforming properties occur when the first of incident signals from the train is stopped, but the subsequent ones may go through the barrier, so the frequency transforming is observed for barriers wider than the penetration depth. For the models of the BZ system the first incident signal is transmitted, but the subsequent ones may be stopped, so the barrier should be narrower than the penetration depth in order to observe frequency transforming.

It is interesting that the frequency transforming for a train of pulses has been already observed experimentally. Agota Toth, Vilmos Gaspar, and Kenneth Showalter[25] studied the excitation of a BZ medium at the end of a capillary tube by a train of pulses propagating inside the capillary. They found that, depending on the capillary's diameter, every arriving pulse may excite the medium (if the capillary is wider) or the excitation never happens (if the diameter is small). However, there is a range of diameters in which the firing number (i.e., the ratio of the excitations of the medium to the number of incoming pulses) is fractional. The capillary's diameter (in ref 25) and the barrier's width (in our case) controls the strength of excitation of the active medium. The firing number in ref 25 has the same meaning as the filtering ratio in our paper. Qualitatively, both results of ref 25 and these presented here mean that there is a range in periodic perturbations of an excitable system in which the system answers in a resonant way. Similar phenomenon observed in a homogeneous reactor was described in refs 26−29.

The authors of ref 25 pointed out that the resonant patterns of transmitted waves may be important in biological systems. They postulated that narrow excitable gaps in an unexcitable tissue may be responsible for transformation in the frequency of a biological signal. Our results show that such gaps are not necessary and the phenomenon may occur if some reagents responsible for signal propagation can diffuse through the unexcitable tissue.

Transformation of chemical signal frequency on a passive barrier has been recently reported by Suzuki, Yoshinobu and Iwasaki, ref 30. The diagram which relates the filtering ratio seen in their experiments with the barrier width and the period of excitations (Figure 10 in ref 30) is in qualitative agreement with our results shown in Figure 7.

Acknowledgment. We are very grateful to Dr. Bartłomiej Legawiec for his advice in the numerical method of solving reaction−diffusion equations used in this study.

References and Notes

(1) Steinbock, O.; Kettunen, P.; Showalter, K. *J. Phys. Chem.* **1996**, *100*, 18970.
(2) Toth, A.; Showalter, K. *J. Chem. Phys.* **1995**, *103*, 2058.
(3) Motoike, I. N.; Yoshikawa, K. *Phys. Rev. E* **1999**, *59*, 5354.
(4) Kusumi, T.; Yamaguchi, T.; Aliev, R. R.; Amemiya, T.; Ohmori, T.; Hashimoto, H.; Yoshikawa, K. *Chem. Phys. Lett.* **1997**, *271*, 355.
(5) Motoike, I. N.; Yoshikawa, K.; Iguchi, Y.; Nakata, S. *Phys. Rev. E* **2001**, *63*, 036220.
(6) Sielewiesiuk, J.; Górecki, J. *Acta Phys. Pol. B* **2001**, *32*, 1589.
(7) Sielewiesiuk, J.; Górecki, J. On the logical function of a cross junction of excitable chemical media. *J. Phys. Chem. A* **2001**, *105*, 8189.
(8) Legawiec, B. Private communication. See also: Legawiec, B.; Ziolkowski, D. *Inz. Chem. Procesowa* **1988**, *2*, 293 (in Polish).
(9) FitzHugh, R. *Biophys. J.* **1961**, *1*, 445.
(10) Nagumo, J. S.; Arimoto, S.; Yoshizawa, S. *Proc. IRE* **1962**, *50*, 2061.
(11) Sielewiesiuk, J.; Górecki, J. Chemical Waves in an Excitable Medium: Their Features and Possible Applications in Information Processing. In *Attractors, Signals and Synergetics. Proceedings of the 1st European Interdisciplinary School on Nonlinear Dynamics for System and Signal Analysis Euroattractor 2000, Warsaw, June 2000*; Wlodzimierz Klonowski, Ed.; Pabst Science Publishers: Lengerich, 2001.
(12) Rovinsky, A. B. *J. Phys. Chem.* **1986**, *90*, 217.

(13) Rovinsky, A. B.; Zhabotinsky, A. M. *J. Phys. Chem.* **1984**, *88*, 6081.
(14) Field, R. J.; Körös, E.; Noyes, R. M. *J. Am. Chem. Soc.* **1972**, *94*, 8649.
(15) Scott, S. K. *Oscillations, Waves and Chaos in Chemical Kinetics*; Oxford University Press: Oxford, U.K., 1994; pp 27−29.
(16) Lazar, A.; Noszticzius, Z.; Försterling, H.-D.; Nagy-Ungvarai, Z. *Physica D* **1995**, *84*, 112.
(17) Zhabotinsky, A. M.; Buchholtz, F.; Kiyatkin, A. B.; Epstein, I. R *J. Phys. Chem.* **1993**, *97*, 7578.
(18) Hammett, L. P. *Physical Organic Chemistry. Reaction Rates, Equilibria and Mechanisms*; McGraw-Hill: New York, 1970.
(19) Aliev, R. R.; Rovinsky, A. B. *J. Phys. Chem.* **1992**, *96*, 732.
(20) Frankowicz, M.; Kawczyñski, A. L.; Górecki, J. *J. Phys. Chem.* **1991**, *95*, 5, 1265.
(21) Miyakawa, K.; Sakamoto, F.; Yoshida, R.; Kokufuta, E.; Yamaguchi, T. *Phys. Rev. E* **2000**, *62*, 793.
(22) Tyson, J. J.; Fife, P. C. *J. Chem. Phys.* **1980**, *73*, 2224.
(23) Dockery, J. D.; Keener, J. P.; Tyson, J. J. *Physica D* **1988**, *30*, 177.
(24) Toth, R.; Papp, A.; Gaspar, V.; Merkin, J. H.; Scott, S. K.; Taylor, A. F. *Phys. Chem. Chem. Phys.* **2001**, *3*, 957.
(25) Toth, A.; Gaspar, V.; Showalter, K. *J. Phys. Chem.* **1994**, *98*, 522.
(26) Dolnik, M.; Finkeova, I.; Schreiber, I.; Marek, M. *J. Phys. Chem.* **1989**, *93*, 2764.
(27) Finkeova, I.; Dolnik, M.; Hrudka, B.; Marek, M. *J. Phys. Chem.* **1990**, *94*, 4110.
(28) Dolnik, M.; Marek, M. *J. Phys. Chem.* **1991**, *95*, 7267.
(29) Dolnik, M.; Marek, M.; Epstein, I. R. *J. Phys. Chem.* **1992**, *96*, 3218.
(30) Suzuki, K.; Yoshinobu, T.; Iwasaki, H. *J. Phys. Chem. A* **2000**, *104*, 5154.